JACS
JOURNAL OF THE AMERICAN CHEMICAL SOCIETY

COMMUNICATION

pubs.acs.org/JACS

A Highly Reactive Mononuclear Non-Heme Manganese(IV)−Oxo Complex That Can Activate the Strong C−H Bonds of Alkanes

Xiujuan Wu,[†] Mi Sook Seo,[†] Katherine M. Davis,[‡] Yong-Min Lee,[†] Junying Chen,[†] Kyung-Bin Cho,[†] Yulia N. Pushkar,*[,‡] and Wonwoo Nam*[,†]

[†]Department of Bioinspired Science, Department of Chemistry and Nano Science, Ewha Womans University, Seoul 120-750, Korea

[‡]Department of Physics, Purdue University, 525 Northwestern Avenue, West Lafayette, Indiana 47907, United States

Supporting Information

ABSTRACT: A mononuclear non-heme manganese(IV)−oxo complex has been synthesized and characterized using various spectroscopic methods. The Mn(IV)−oxo complex shows high reactivity in oxidation reactions, such as C−H bond activation, oxidations of olefins, alcohols, sulfides, and aromatic compounds, and N-dealkylation. In C−H bond activation, the Mn(IV)−oxo complex can activate C−H bonds as strong as those in cyclohexane. It is proposed that C−H bond activation by the non-heme Mn(IV)−oxo complex does not occur via an oxygen-rebound mechanism. The electrophilic character of the non-heme Mn(IV)−oxo complex is demonstrated by a large negative ρ value of −4.4 in the oxidation of *para*-substituted thioanisoles.

High-valent metal−oxo species have been invoked as key intermediates in the oxidation of organic substrates by metalloenzymes and metal catalysts.[1] A number of high-valent metal−oxo complexes have been synthesized and characterized using various spectroscopic methods and X-ray crystallography, and their reactivities have been investigated extensively in the oxidation of organic substrates, including C−H bond activation and oxygen atom transfer (OAT) reactions.[2] Some examples are synthetic heme and non-heme iron−oxo complexes as chemical models of cytochromes P450 and non-heme iron enzymes, respectively, and mechanisms of OAT from iron−oxo complexes to organic substrates have been intensively investigated in various oxidation reactions.[3]

High-valent manganese−oxo complexes bearing heme and non-heme ligands have also attracted much attention in the communities of bioinorganic and oxidation chemistry, since they have shown promise as plausible intermediates in the catalytic oxidation of organic substrates by manganese catalysts and in water splitting by Photosystem II.[4,5] However, synthetic manganese−oxo complexes have shown much less reactivity than their iron−oxo analogues in oxidation reactions,[6−8] especially in non-heme manganese−oxo cases. For example, while it has been shown that non-heme iron(IV)−oxo complexes are able to activate C−H bonds of unactivated alkanes [e.g., cyclohexane, which has a C−H bond dissociation energy (BDE) of 99.5 kcal mol^{-1}],[9] the non-heme manganese(IV)−oxo complexes reported to date are capable of activating weak C−H bonds of activated alkanes (e.g., alkylaromatics such as xanthene, 9,10-dihydroanthracene, and fluorene).[7] In addition, while it has been well-established that the C−H bond activation of alkanes by iron−oxo complexes occurs via an oxygen-rebound mechanism,[10] the mechanism of C−H bond activation by manganese−oxo analogues has been less clearly understood and remains elusive. This is probably due to the low reactivity of the manganese−oxo complexes in C−H bond activation reactions. In this communication, we report the synthesis, characterization, and results of reactivity studies of a highly reactive non-heme manganese(IV)−oxo complex that can activate C−H bonds as strong as those in cyclohexane. The mechanism of the C−H bond activation by the non-heme manganese(IV)−oxo complex is discussed as well. In addition to C−H bond activation, the manganese−oxo complex turns out to be a versatile oxidant in the oxidation of olefins, alcohols, sulfides, and aromatic compounds as well as in N-dealkylation.

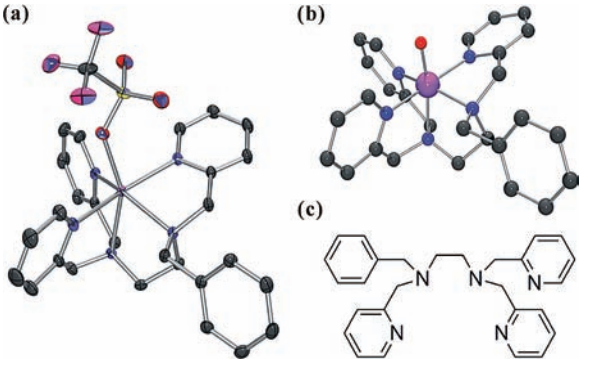

Figure 1. (a) X-ray structure of $[Mn^{II}(Bn\text{-}TPEN)(CF_3SO_3)]^+$ (**1**−CF_3SO_3), showing 30% probability thermal ellipsoids. Crystallographic and structural data are listed in Tables S1 and S2. (b) DFT-optimized solution-phase structure of **2** calculated at the B3LYP/LACVP level. The Mn−O bond length was calculated to be 1.68 Å (see the DFT Calculations Section in the SI for computational details). H atoms have been omitted for clarity (Mn, purple; N, blue; O, red; C, black; S, yellow; F, pink). (c) Structure of the Bn-TPEN ligand.

The starting manganese(II) complex, $[Mn(II)(Bn\text{-}TPEN)]^{2+}$ (**1**) [Bn-TPEN = *N*-benzyl-*N*,*N*′,*N*′-tris(2-pyridylmethyl)-1,2-diaminoethane], was synthesized by reacting $Mn^{II}(CF_3SO_3)_2 \cdot 2CH_3CN$ with a pentadentate Bn-TPEN ligand in CH_3CN under an Ar atmosphere [see the Experimental Section and Figure S1 in the Supporting Information (SI) for synthetic procedures and spectroscopic characterization]. The crystal structure of **1**−CF_3SO_3 exhibits a distorted octahedral geometry

Received: September 9, 2011
Published: November 17, 2011

dx.doi.org/10.1021/ja208523u | *J. Am. Chem. Soc.* 2011, 133, 20088–20091

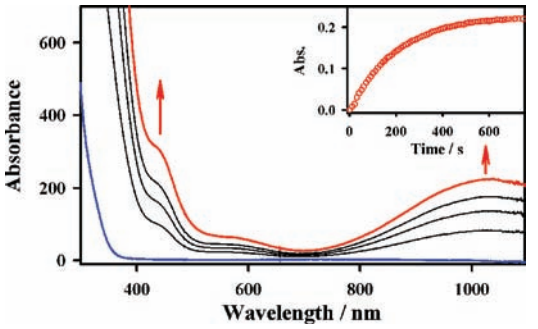

Figure 2. UV−vis spectral changes showing the formation of **2** (red line) in the reaction of $[Mn(II)(Bn\text{-}TPEN)]^{2+}$ (1 mM, blue line) and PhIO (4 mM in CF_3CH_2OH) in CF_3CH_2OH at 25 °C. The inset shows the time course of the formation of **2** monitored at 1040 nm.

(Figure 1a and Tables S1 and S2 in the SI). Addition of 4 equiv of iodosylbenzene (PhIO) to a 1 mM solution of **1** in CF_3CH_2OH at 25 °C gave a greenish-yellow complex, **2**, with an absorption band at 1040 nm ($\varepsilon \approx 220\ M^{-1}\ cm^{-1}$) and shoulders at 450 and 610 nm (Figure 2). The metastable intermediate ($t_{1/2} \approx 40$ min at 25 °C) was characterized using various spectroscopic techniques. The X-band EPR spectrum of **2** shows signals at $g = 5.5$, 2.76, and 1.76, characteristic of $S = {}^3/_2$ Mn^{IV} (Figure S2).[7a,d,g] The spin state of **2** was confirmed using the Evans' NMR method,[11] and the magnetic moment of $4.3\mu_B$ indicates the spin state of $S = {}^3/_2$ for **2**. The electrospray ionization mass spectrometry (ESI-MS) data for **2** show two prominent ion peaks at m/z 247.0 and 643.0 (Figure S3), whose mass and isotope distribution patterns correspond to $[Mn^{IV}(O)(Bn\text{-}TPEN)]^{2+}$ (calcd m/z 247.0) and $[Mn^{IV}(O)(Bn\text{-}TPEN)(CF_3SO_3)]^{+}$ (calcd m/z 643.1). Upon introduction of ^{18}O into **2** using $PhI^{18}O$, shifts from m/z 247.0 to 248.0 and m/z 643.0 to 645.0 were observed (Figure S3), indicating that **2** contains an oxygen atom.

X-ray absorption spectroscopy (XAS) at the Mn K edge confirmed the assignment of the oxidation states of Mn ions in the studied manganese complexes. The Mn K edges show a pronounced shift toward higher energies in the series containing Mn^{II} (**1**), Mn^{III} (**3**) (see below), and Mn^{IV} (**2**) (Figure 3a). The relatively intense pre-edge feature at 6541.6 eV for **2** indicates distortion of the octahedral environment with possible lowering of the symmetry (also see Table S3 and Figure S4). The extended X-ray absorption fine structure (EXAFS) data in Figure 3b show a considerable difference in structure between **1** and **2**. The first EXAFS peak, corresponding to Mn−O,N interactions in the first coordination sphere, is shifted to a shorter apparent distance in **2**. This change can be rationalized in terms of a shortening of the Mn−O,N bond distances in **2**, and fits to the EXAFS data indeed indicated the presence of a 1.69 Å Mn═O interaction as well as shortening of the Mn−N distance (Table S3; also see the 1.68 Å Mn−O distance obtained from the density functional theory (DFT) calculations in Figure 1b and the DFT Calculations Section). This Mn−O distance is comparable to the distances of 1.68 and 1.58 Å reported for five-coordinate Mn(IV)(O) complexes[12] but shorter than the distances of 1.77 and 1.84 Å in six-coordinate Mn(IV) complexes.[13]

The reactivity of **2** in C−H bond activation of hydrocarbons at 25 °C was investigated. Upon addition of ethylbenzene to a solution of **2**, the intermediate was converted to a new species, **3**, with isosbestic points at 405 and 730 nm (Figure 4a). The first-order rate constant, determined by pseudo-first-order fitting of

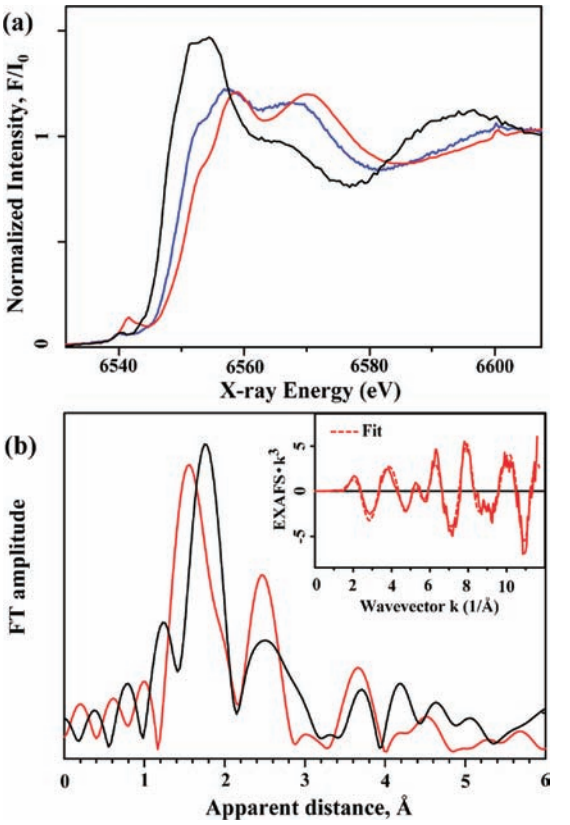

Figure 3. (a) Normalized Mn K-edge XAS of $[Mn^{II}(Bn\text{-}TPEN)]^{2+}$ (**1**, black line), $Mn^{IV}(O)(Bn\text{-}TPEN)]^{2+}$ (**2**, red line), and $[Mn^{III}(Bn\text{-}TPEN)(OCH_2CF_3)]^{2+}$ (**3**, blue line). (b) Overlay of the Fourier transforms ($k = 3.5-11.3$ $Å^{-1}$) of **1** (black line) and **2** (red line). The inset shows EXAFS data for **2** with the fit (Table S3).

the kinetic data for the decay of **2** (Figure 4a inset), increased linearly with increasing ethylbenzene concentration (Figure S5), giving a second-order rate constant of $2.7 \times 10^{-2}\ M^{-1}\ s^{-1}$ at 25 °C. A kinetic isotope effect (KIE) value of 7.9(3) was obtained in the oxidation of ethylbenzene by **2** (Figure S5). Similarly, the second-order rate constants were determined for the oxidation of other substrates by **2**, and a linear correlation between the reaction rate and the C−H BDE of the substrate was found (Figure 4b and Table S4 and Figure S6). On the basis of the large KIE value and the good correlation between the reaction rate and the substrate BDE, we conclude that H-atom abstraction from a C−H bond of the substrate by **2** is the rate-determining step (r.d.s.) in the C−H bond activation reaction.

Product analysis of the reaction solution of the ethylbenzene oxidation by **2** revealed the formation of 1-phenylethanol (23 ± 4%), acetophenone (12 ± 3%), and styrene (7 ± 3%).[14] The latter is the product of a desaturation reaction.[15] When the ethylbenzene oxidation was performed with ^{18}O-labeled **2** (**2**-^{18}O), the oxygens in the phenylethanol and acetophenone products were found to derive from the manganese−oxo species (Figure S7).[14] We also characterized **3**, the decay product of **2** in the ethylbenzene oxidation (see Figure 4a) using various spectroscopic methods. ESI-MS of **3** showed prominent peaks at m/z 288.5 and 725.9 (Figure S8) whose mass and isotope distribution patterns correspond to $[Mn^{III}(Bn\text{-}TPEN)(CF_3CH_2O)]^{2+}$ (calcd m/z 288.5) and $[Mn^{III}(Bn\text{-}TPEN)(CF_3CH_2O)(CF_3SO_3)]^{+}$ (calcd m/z 726.0), respectively. The X-band EPR spectrum of

dx.doi.org/10.1021/ja208523u | J. Am. Chem. Soc. 2011, 133, 20088–20091

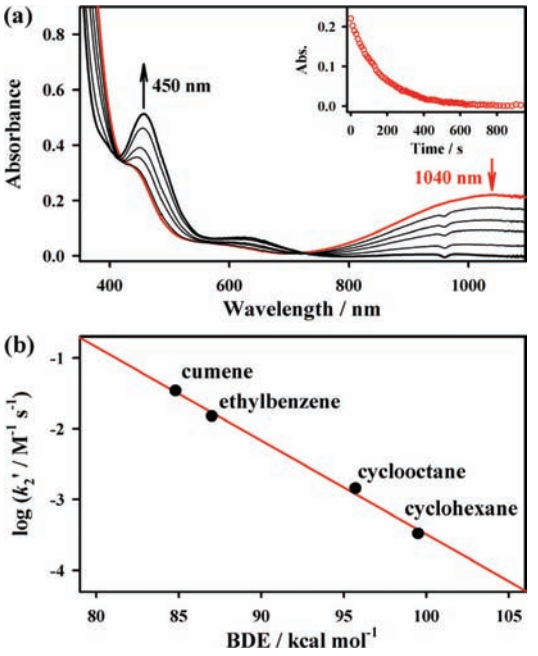

Figure 4. (a) UV−vis spectral changes of **2** (1 mM, red line) upon addition of ethylbenzene (200 mM) in 19:1 (v/v) CF_3CH_2OH/CH_3CN at 25 °C. The inset shows the time course of the decay of **2** monitored at 1040 nm. (b) Plot of log k_2' for **2** against the substrate C−H BDE. The second-order rate constants k_2 were determined at 25 °C and then adjusted for reaction stoichiometry to yield k_2' values based on the number of equivalent target C−H bonds in the substrate (see Table S4 and Figure S6).

Scheme 1. Proposed Mechanism for the Activation of C−H Bonds by $[Mn^{IV}(O)(Bn\text{-}TPEN)]^{2+}$ (2) (L and R′OH Stand for the Bn-TPEN Ligand and the CF_3CH_2OH Solvent, Respectively)

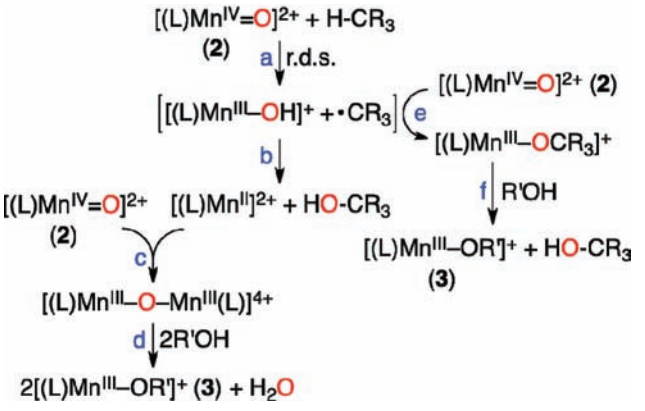

3 was silent, suggesting the oxidation state of +3 for the Mn ion in **3**, which is consistent with the position of the Mn K edge of **3** (see Figure 3a). Compound **3** was prepared independently by reacting **1** and peracetic acid or from the natural decay of **2** in CF_3CH_2OH; **3** prepared in these reactions showed spectral data identical to those of **3** obtained in the oxidation of ethylbenzene by **2** (see Figures S9 and S10 for UV−vis, ESI-MS, and EPR spectroscopic data and Figure 3a for XAS data). On the basis of these spectroscopic studies, **3** has been assigned as $[Mn(III)(Bn\text{-}TPEN)(OCH_2CF_3)]^{2+}$.

Table 1. Rate Constants Determined for the Oxidation of Substrates by 2[a]

reaction	substrate	k_2 (M^{-1} s^{-1})
C−H bond activation	ethylbenzene	2.7×10^{-2}
alkene oxidation	cyclohexene	3.2×10^{-1}
alcohol oxidation	benzyl alcohol	4.9×10^{-2}
aromatic oxidation	naphthalene	9.4×10^{-2}
S-oxidation[b]	thioanisole	1.3
N-dealkylation	*N*,*N*-dimethylaniline	N.D.[c]

[a] Reaction conditions: **2** (1 mM) in 19:1 (v/v) CF_3CH_2OH/CH_3CN at 25 °C. [b] The reaction temperature was 0 °C. [c] The reaction was too fast for the rate constant to be determined, even at −20 °C.

It is of interest to note that the one-electron-reduced Mn(III) complex **3** rather than the two-electron-reduced Mn(II) complex was formed in the C−H bond activation reactions by Mn(IV)−oxo complex **2**. This observation is contrary to the well-known oxygen-rebound mechanism; the hydroxylation of alkanes by an iron(IV)−oxo porphyrin π-cation radical affords an iron(III) porphyrin complex as a two-electron-reduced product.[10] The formation of Mn(III) complexes in C−H bond activation by non-heme Mn(IV)−oxo complexes has also been reported recently by Borovik, Costas, and their co-workers.[7d,g] How then are the Mn(III) complexes formed instead of Mn(II) complexes in the C−H bond activation reactions by Mn(IV)−oxo complexes? A proposed mechanism is depicted in Scheme 1. The first step of the C−H bond activation is H-atom abstraction from a C−H bond of the substrate by **2** (step a), which is the rate-determining step, as we have shown above. The rebound of the hydroxyl group to the alkyl radical generates a Mn(II) complex and a hydroxylation product (step b), and this is followed by a reaction between the Mn(II) complex and **2** that affords first a μ-oxo-bridged Mn(III) dimer (step c) and then Mn(III) complex **3** (step d). To test this proposed mechanism, we reacted equal amounts of **2** and $[Mn(II)(Bn\text{-}TPEN)]^{2+}$ under the conditions for the C−H bond activation reaction (e.g., 25 °C in CF_3CH_2-OH). However, the formation of **3** was not observed (Figure S11), leading us to conclude that **3** is not the product of the reaction of a Mn(II) complex and **2**. An alternative pathway for the formation of **3** would be the coupling of the alkyl radical with another molecule of **2**, yielding **3** and the hydroxylation product (Scheme 1, steps e and f). We propose at this moment that the reaction between the Mn(III)−OH and alkyl radical species is relatively slow because of a significant energy barrier in the oxygen-rebound step (step b),[16] allowing a fast reaction between the alkyl radical and **2** to occur, giving **3** as a product (step e). Detailed investigations, including DFT calculations, are underway to understand the mechanism of the C−H bond activation by non-heme Mn(IV)−oxo complexes.

The reactivity of **2** was investigated kinetically in other oxidation reactions (Table 1), in view of the precedent that non-heme iron(IV)−oxo complexes are versatile oxidants in those oxidation reactions.[17] In all of the reactions, **2** showed a high reactivity comparable to those of non-heme iron(IV)−oxo complexes (Table 1 and Figure S12). In addition, as observed in the oxidation of sulfides by non-heme iron(IV)−oxo complexes,[17c] the electrophilic character of the non-heme Mn(IV)−oxo complex was demonstrated by a large negative ρ value of −4.4 in the oxidation of para-substituted thioanisoles (Figure S13). Interestingly, in contrast to the C−H bond activation reactions, **2** was not converted to the Mn(III) complex **3** but to the Mn(II)

complex (Figure S14), indicating that the oxidation of sulfides by **2** occurs via a two-electron oxidation process. In other oxidation reactions, such as in the oxidation of olefins, alcohols, and aromatic compounds, we observed the formation of **3** via one-electron oxidation process (data not shown). Although we have reported preliminary results that non-heme Mn(IV)−oxo complex **2** is a versatile oxidant in the oxidation of a variety of substrates via one- versus two-electron oxidation processes, detailed studies are underway to elucidate the mechanisms of the oxidation of the substrates by mononuclear non-heme manganese(IV)−oxo complexes.

■ ASSOCIATED CONTENT

Supporting Information. Experimental and DFT details, Tables S1−S7, and Figures S1−S14. This material is available free of charge via the Internet at http://pubs.acs.org.

■ AUTHOR INFORMATION

Corresponding Author
ypushkar@purdue.edu; wwnam@ewha.ac.kr

■ ACKNOWLEDGMENT

The research at EWU was supported by GRL (2010-00353) and WCU (R31-2008-000-10010-0). The research at Purdue was supported by the Department of Energy, Office of Basic Energy Sciences (DOE-BES) (DE-FG02-10ER16184 to Y.P.) and an NSF Graduate Research Fellowship under Grant 0833366 (K.M.D.). Synchrotron facilities were provided by the Advanced Photon Source (APS) at Argonne National Laboratory, operated by DOE-BES under Contract No. DE-AC02-06CH11357. We thank Dr. Steve Heald and Dr. Dale Brewer for help with experiments at Beamline BM-20, APS.

■ REFERENCES

(1) (a) Ortiz de Montellano, P. R. *Cytochrome P450: Structure, Mechanism, and Biochemistry*, 3rd ed.; Kluwer: New York, 2005. (b) Abu-Omar, M. M.; Loaiza, A.; Hontzeas, N. *Chem. Rev.* **2005**, *105*, 2227. (c) Krebs, C.; Fujimori, D. G.; Walsh, C. T.; Bollinger, J. M., Jr. *Acc. Chem. Res.* **2007**, *40*, 484. (d) Green, M. T. *Curr. Opin. Chem. Biol.* **2009**, *13*, 84. (e) Ortiz de Montellano, P. R. *Chem. Rev.* **2010**, *110*, 932. (f) Shaik, S.; Lai, W.; Chen, H.; Wang, Y. *Acc. Chem. Res.* **2010**, *43*, 1154.

(2) (a) Mayer, J. M. *Acc. Chem. Res.* **2011**, *44*, 36. (b) Borovik, A. S. *Chem. Soc. Rev.* **2011**, *40*, 1870. (c) Gunay, A.; Theopold, K. H. *Chem. Rev.* **2010**, *110*, 1060. (d) Warren, J. J.; Tronic, T. A.; Mayer, J. M. *Chem. Rev.* **2010**, *110*, 6961. (e) Stone, K. L.; Borovik, A. S. *Curr. Opin. Chem. Biol.* **2009**, *13*, 114.

(3) (a) Abu-Omar, M. M. *Dalton Trans.* **2011**, *40*, 3435. (b) Bruijnincx, P. C. A.; van Koten, G.; Klein Gebbink, R. J. M. *Chem. Soc. Rev.* **2008**, *37*, 2716. (c) van Eldik, R. *Coord. Chem. Rev.* **2007**, *251*, 1649. (d) Groves, J. T. *J. Inorg. Biochem.* **2006**, *100*, 434.

(4) (a) Meunier, B.; Robert, A.; Pratviel, G.; Bernadou, J. In *The Porphyrin Handbook*; Kadish, K. M., Smith, K. M., Guilard, R., Eds.; Academic Press: San Diego, 2000; Vol. 4, Chapter 31, pp 119−187. (b) Murphy, A.; Dubois, G.; Stack, T. D. P. *J. Am. Chem. Soc.* **2003**, *125*, 5250. (c) Nehru, K.; Kim, S. J.; Kim, I. Y.; Seo, M. S.; Kim, Y.; Kim, S.-J.; Kim, J.; Nam, W. *Chem. Commun.* **2007**, 4623. (d) Terry, T. J.; Stack, T. D. P. *J. Am. Chem. Soc.* **2008**, *130*, 4945.

(5) (a) McEvoy, J. P.; Brudvig, G. W. *Chem. Rev.* **2006**, *106*, 4455. (b) Meyer, T. J.; Huynh, M. H. V.; Thorp, H. H. *Angew. Chem., Int. Ed.* **2007**, *46*, 5284. (c) Pecoraro, V. L.; Hsieh, W.-Y. *Inorg. Chem.* **2008**, *47*, 1765. (d) Romain, S.; Vigara, L.; Llobet, A. *Acc. Chem. Res.* **2009**, *42*, 1944.

(6) Manganese−oxo porphyrins: (a) Groves, J. T.; Lee, J.; Marla, S. S. *J. Am. Chem. Soc.* **1997**, *119*, 6269. (b) Jin, N.; Ibrahim, M.; Spiro, T. G.; Groves, J. T. *J. Am. Chem. Soc.* **2007**, *129*, 12416. (c) Song, W. J.; Seo, M. S.; George, S. D.; Ohta, T.; Song, R.; Kang, M.-J.; Tosha, T.; Kitagawa, T.; Solomon, E. I.; Nam, W. *J. Am. Chem. Soc.* **2007**, *129*, 1268. (d) Lee, J. Y.; Lee, Y.-M.; Kotani, H.; Nam, W.; Fukuzumi, S. *Chem. Commun.* **2009**, 704.

(7) Non-heme manganese−oxo complexes: (a) Parsell, T. H.; Behan, R. K.; Green, M. T.; Hendrich, M. P.; Borovik, A. S. *J. Am. Chem. Soc.* **2006**, *128*, 8728. (b) Yin, G.; Danby, A. M.; Kitko, D.; Carter, J. D.; Scheper, W. M.; Busch, D. H. *J. Am. Chem. Soc.* **2007**, *129*, 1512. (c) Yin, G.; Danby, A. M.; Kitko, D.; Carter, J. D.; Scheper, W. M.; Busch, D. H. *J. Am. Chem. Soc.* **2008**, *130*, 16245. (d) Parsell, T. H.; Yang, M.-Y.; Borovik, A. S. *J. Am. Chem. Soc.* **2009**, *131*, 2762. (e) Kurahashi, T.; Kikuchi, A.; Shiro, Y.; Hada, M.; Fujii, H. *Inorg. Chem.* **2010**, *49*, 6664. (f) Sawant, S. C.; Wu, X.; Cho, J.; Cho, K.-B.; Kim, S. H.; Seo, M. S.; Lee, Y.-M.; Kubo, M.; Ogura, T.; Shaik, S.; Nam, W. *Angew. Chem., Int. Ed.* **2010**, *49*, 8190. (g) Garcia-Bosch, I.; Company, A.; Cady, C. W.; Styring, S.; Browne, W. R.; Ribas, X.; Costas, M. *Angew. Chem., Int. Ed.* **2011**, *50*, 5648.

(8) Corrole and corrolazine manganese−oxo complexes: (a) Prokop, K. A.; de Visser, S. P.; Goldberg, D. P. *Angew. Chem., Int. Ed.* **2010**, *49*, 5091. (b) Han, Y.; Lee, Y.-M.; Mariappan, M.; Fukuzumi, S.; Nam, W. *Chem. Commun.* **2010**, *46*, 8160. (c) Kumar, A.; Goldberg, I.; Botoshansky, M.; Buchman, Y.; Gross, Z. *J. Am. Chem. Soc.* **2010**, *132*, 15233. (d) Fukuzumi, S.; Kotani, H.; Prokop, K. A.; Goldberg, D. P. *J. Am. Chem. Soc.* **2011**, *133*, 1859.

(9) (a) Kaizer, J.; Klinker, E. J.; Oh, N. Y.; Rohde, J.-U.; Song, W. J.; Stubna, A.; Kim, J.; Münck, E.; Nam, W.; Que, L., Jr. *J. Am. Chem. Soc.* **2004**, *126*, 472. (b) Seo, M. S.; Kim, N, H.; Cho, K.-B.; So, J. E.; Park, S. K.; Clémancey, M.; Garcia-Serres, R.; Latour, J.-M.; Shaik, S.; Nam, W. *Chem. Sci* **2011**, *2*, 1039.

(10) (a) Groves, J. T.; McClusky, G. A. *J. Am. Chem. Soc.* **1976**, *98*, 859. (b) Ortiz de Montellano, P. R.; Stearns, R. A. *J. Am. Chem. Soc.* **1987**, *109*, 3415. (c) Schöneboom, J. C.; Cohen, S.; Lin, H.; Shaik, S.; Thiel, W. *J. Am. Chem. Soc.* **2004**, *126*, 4017. (d) Hirao, H.; Kumar, D.; Que, L., Jr.; Shaik, S. *J. Am. Chem. Soc.* **2006**, *128*, 8590.

(11) Evans, D. F. *J. Chem. Soc.* **1959**, 2003.

(12) (a) Ayougou, K.; Bill, E.; Charnock, J. M.; Garner, C. D.; Mandon, D.; Trautwein, A. X.; Weiss, R.; Winkler, H. *Angew. Chem., Int. Ed. Engl.* **1995**, *34*, 343. (b) Kurahashi, T.; Kikuchi, A.; Tosha, T.; Shiro, Y.; Kitagawa, T.; Fujii, H. *Inorg. Chem.* **2008**, *47*, 1674.

(13) (a) Bortolini, O.; Meunier, B.; Friant, P.; Ascone, I.; Goulon, J. *New J. Chem.* **1986**, *10*, 39. (b) Lassalle-Kaiser, B.; Hureau, C.; Pantazis, D. A.; Pushkar, Y.; Guillot, R.; Yachandra, V. K.; Yano, J.; Neese, F.; Anxolabéhère-Mallart, E. *Energy Environ. Sci.* **2010**, *3*, 924.

(14) Hull, J. F.; Balcells, D.; Sauer, E. L. O.; Raynaud, C.; Brudvig, G. W.; Crabtree, R. H.; Eisenstein, O. *J. Am. Chem. Soc.* **2010**, *132*, 7605.

(15) The product distribution and yields were different when the reaction was carried out in the presence of O_2. Similarly, the source of oxygen in the oxygenated products was molecular oxygen in this reaction, not the Mn(IV)−oxo complex (see Figure S7 for a detailed discussion).

(16) Preliminary DFT calculations suggested that there is a significant activation barrier for the rebound of the hydroxyl group to the alkyl radical (Scheme 1, step b), which would constitute a rate-limiting step if the reaction indeed were to proceed by this route.

(17) (a) Lim, M. H.; Rohde, J.-U.; Stubna, A.; Bukowski, M. R.; Costas, M.; Ho, R. Y. N.; Münck, E.; Nam, W.; Que, L., Jr. *Proc. Natl. Acad. Sci. U.S.A.* **2003**, *100*, 3665. (b) Oh, N. Y.; Suh, Y.; Park, M. J.; Seo, M. S.; Kim, J.; Nam, W. *Angew. Chem., Int. Ed.* **2005**, *44*, 4235. (c) Park, M. J.; Lee, J.; Suh, Y.; Kim, J.; Nam, W. *J. Am. Chem. Soc.* **2006**, *128*, 2630. (d) Nehru, K.; Seo, M. S.; Kim, J.; Nam, W. *Inorg. Chem.* **2007**, *46*, 293. (e) de Visser, S. P.; Oh, K.; Han, A.-R.; Nam, W. *Inorg. Chem.* **2007**, *46*, 4632.